

User Association and Interference Management in Massive MIMO HetNets

Qiaoyang Ye, Ozgun Y. Bursalioglu, Haralabos C. Papadopoulos, Constantine
Caramanis and Jeffrey G. Andrews

Abstract

Two key traits of 5G cellular networks are much higher base station (BS) densities – especially in the case of low power BSs – and the use of massive MIMO at these BSs. This paper explores how massive MIMO can be used to jointly maximize the offloading gains and minimize the interference challenges arising from adding small cells. We consider two interference management approaches: *joint transmission* (JT) with local precoding, where users are served simultaneously by multiple BSs without requiring channel state information exchanges among cooperating BSs, and *resource blanking*, where some macro BS resources are left blank to reduce the interference in small cells. A key advantage of massive MIMO is that the instantaneous rates do not depend on small scale fading, and can be predicted *a priori*. This allows us to develop a unified network utility maximization (NUM) problem for JT and blanking, which optimizes resource allocations to improve the rate of cell-edge users. We propose an efficient dual subgradient based algorithm, which converges towards the NUM solution. A scheduling scheme is also proposed to approach the NUM solution. Simulations illustrate more than $2\times$ rate gain for the 10th percentile users vs. an optimal association without interference management.

I. INTRODUCTION

Two key trends in cellular network evolution are the increasing densification and heterogeneity in base station (BS) deployments [1], and the introduction of ever-larger antenna arrays. Smart ultra-densification and massive MIMO are considered as two of the most important technologies in 5G cellular systems [2, 3]¹. The massive MIMO regime is the setting when the number of antennas at a BS is significantly

Q. Ye, C. Caramanis and J. G. Andrews are with WNCG, The University of Texas at Austin, Austin, TX, USA, O. Y. Bursalioglu and H. C. Papadopoulos are with Docomo Innovations Inc, Palo Alto, CA, USA. Email: qye@utexas.edu, {obursalioglu, hpapadopoulos}@docomoinnovations.com, constantine@utexas.edu, jandrews@ece.utexas.edu. Manuscript last revised: November 10, 2018.

¹As higher-frequency spectrum being available, large arrays become practical even for small cells. For example, at 3.5GHz band, a 36-antenna (arranged on a square grid at half-wavelength separation) can be implemented on a 26cm \times 26cm surface. The required implementation area would be smaller as the carrier frequency becomes higher.

larger than the number of users that are simultaneously served by the BS [4–6]. In this paper, various aspects such as user association, load balancing, scheduling, and interference management are considered for future network scenarios with massive MIMO deployments where these technologies are adapted together.

A. Motivation and Related Work

Conventionally, mobile user equipments (UEs) are served by the BS providing the largest signal-to-interference-plus-noise ratio (SINR) or the largest received power [7] – called *max-SINR association* in this paper. In heterogeneous networks (HetNets), however, different types of BSs can have large disparities in transmit power, so a max-SINR association results in heavily congested macrocell BSs and lightly loaded low-power small cell BSs. This results in a very inefficient use of available time-frequency resources, and strongly motivates load balancing, which in effect means pushing some UE traffic onto lightly loaded small cells even if it requires reducing their SINRs by many dBs [8].

Load Balancing. Several approaches have been used to study load balancing in HetNets, including stochastic geometry [9, 10], game theory [11], and system-level simulations [12, 13]. Meanwhile, in industry, proactive load balancing is accomplished by *biasing* UE association towards the small cells [12, 13]². Our initial study on load balancing [14] formulated a network utility maximization (NUM) problem for user association in HetNets with single-antenna BSs, where the resources are equally allocated among users in the same cell. We showed in [14] that the simple biasing approach with carefully designed bias values can perform surprisingly close to the optimal performance. One shortcoming of [14] is that the equal resource allocation can be suboptimal if the user associations happen on a much slower time scale than the channel variations. In general, the user association and scheduling (resource allocation) problems are coupled, and it is quite difficult to jointly optimize them.

Massive MIMO. A key benefit of massive MIMO is that the extra diversity afforded by the large antenna array averages out the fast fading, and thus the instantaneous rate stabilizes to the longer-term mean. This rate is of course still subject to changes in path loss and shadowing, but these happen on much slower time scales. As shown in [15], the instantaneous rates can be predicted with peak-rate proxies, which are independent of scheduled instances and user sets. This property allows the decoupling of user association and scheduling, which is exploited to achieve near-optimal load balancing in massive

²Biasing can be commonly done as follows: by artificially adding a bias value (e.g., 10 dB) to received signal power from small cell layer at UEs

MIMO HetNets using simple user-BS association methods with cellular transmission (where data for each user is transmitted from a single BS) [15].

Coordinated multi-point transmission. MIMO techniques also provide the option of serving a user at high rates from multiple BSs – referred to as coordinated multi-point transmission (CoMP), which is proposed as one of the core features in LTE-Advanced [16–18]. The set of BSs that cooperatively serve the same user is called a *BS cluster*. Paper [19] studies how to determine the BS clusters, while [20–22] investigate the joint design involving some of the following aspects: BS cluster selection, beamforming, user scheduling and power allocation. In this paper, we consider CoMP as a means for improving network performance, in particular, the bottom (e.g., 10th percentile) long-term rate. CoMP is naturally enabled by reciprocity-based training, since a single uplink pilot from a user can train all nearby antennas. In regular layouts with massive MIMO BSs, [23] shows gains to cell-edge users via CoMP. In this paper, we focus on a distributed-MIMO form of CoMP, which allows local precoding at each BS and does not require channel state information (CSI) exchanges among cooperating BSs. We call this specific form of CoMP as Joint Transmission (JT). JT allows us to develop a systematic resource allocation approach for CoMP (and cellular transmission as a special case).

Resource Blanking. As the macrocells that users are offloaded from now become strong interferers for these offloaded users, the increased interference eats into the gains offered by load balancing. This motivates us to jointly consider user association and interference management, to improve the performance of low-SINR (i.e., “cell edge”) users. Besides CoMP, another popular interference management approach is to leave some macro resource blocks (RBs) blank, similar to enhanced intercell interference coordination (eICIC) in 3GPP [24]. The key difference between RB blanking in our work and eICIC is that eICIC focuses on the time domain, while in this work blanking is applied on both time and frequency domains. We call the RBs where macro BSs are muted the *blank RBs*, while the rest of RBs are called *normal RBs*. Several works have considered the joint problem of user association and RB blanking. For example, [25] proposes a dynamic approach adapting the muting duty cycle to load variations, while [26–30] consider a more static approach.

The joint optimization of user association and interference management is still an open issue in massive MIMO HetNets. We tackle this issue by developing a unified framework for HetNets with both JT and RB blanking capability. Other interference management approaches can also be adopted, but at the cost of overhead, complexity or/and intractability (e.g., schemes with joint precoding [18]). Study

of more general interference management techniques (see, e.g., [31]) are beyond the scope of this work.

Cross-layer Optimization. To study the joint user association and interference management problem, we propose to use the cross-layer optimization approach, aiming to improve the rate distribution, particularly the cell-edge performance. Cross-layer optimization is a very popular approach to study the resource allocation problems in wireless networks (see, e.g., [32, 33] and references therein). Among these, the work most related to the goal of this paper is [22], which investigates the BS clustering and user scheduling problems with disjoint clusters (i.e., each BS belongs to at most one cluster on any RB). Our framework different from [22] in that it can be applied to not only the cases with disjoint clusters, but also more flexible cases where a BS may belong to different clusters on the same RBs, and different users can be served by different clusters (i.e., user-specific clusters). To the best of our knowledge, this is the first work proposing a framework to jointly design user-specific clusters and resource allocation to maximize the utility in massive MIMO HetNets.

Most existing literature studies the user scheduling problem slot by slot leveraging the gradient algorithm proposed in [34]. However, due to the fact that BSs can belong to different clusters and resource constraints cross over different clusters, it is difficult to transform our problem in each slot to some typical types of polynomial-time solvable problems (e.g., the max weight matching problem [35–37]). Moreover, it is quite difficult to efficiently obtain the achievable optimal utility in the gradient algorithm (e.g., [22]). Alternatively, the methods we develop are based on formulating a NUM problem for user association and resource allocation via extensions of the cellular transmission framework in [15]. Solving the NUM problem provides the desired average resource allocation – defined later in Sec. III-B as *activity fractions*. We then present scheduling policies at a finer time scale (i.e., RB level) to approach the optimized (coarser time scale) resource allocation.

B. Contributions and Organization

In this paper, we present a novel framework for the joint optimization of user association and interference management in massive MIMO HetNets, resulting in the following main contributions.

A unified NUM problem. By exploiting the predictable instantaneous rate, user association and scheduling problems can be decoupled, allowing us in Sec. IV to formulate a unified convex optimization problem for resource allocation with both JT and RB blanking. Note that in the considered JT, the clusters are user-specific (i.e., different users can be served by different clusters). The formulated NUM problem can also be applied to scenarios where some bandwidth resources are explicitly reserved for macro or

small cell operation while some resources are reserved for being shared by both layers. As an extension of [15], the optimal solutions can always be realized by a suitably designed scheduler when blanking is used in cellular transmission. On the other hand, with JT, we show that there exist some solutions that are not implementable. Naturally, the solution of the NUM problem – called the *NUM solution* – upper bounds the network performance and can serve as a useful benchmark.

Dual subgradient based algorithm. Sec. V presents an efficient algorithm based on the dual subgradient method, which converges towards the optimal dual variables. As the objective function is not strictly convex, it is difficult to get the optimal primal variables given optimal dual variables. Exploring the solution structure, we formulate a small-size linear program (LP) to get the optimal primal variables.

Simple scheduling scheme to approach the NUM solution. In Sec. VI, we also present scheduling policies at a finer time scale (i.e., RB level), which target approaching the optimized (coarser time scale) resource allocations obtained by solving the NUM problem.

Simulations³ in Sec. VII show that the proposed harmonized CoMP/cellular operation can provide significant gains with respect to cellular-only massive MIMO operation [15], especially for low-rate users. For example, the rate of bottom (10th percentile) users in our setup is about $2.2\times$ with respect to the optimal user association without interference management, which itself is much larger than the max-SINR association. The dual subgradient based algorithm approaches the NUM solution. Also, the utility provided by the proposed scheduling scheme is within 90% of the utility provided by the NUM solution.

II. SYSTEM MODEL

In this paper, we focus on delay-tolerant best-effort traffic. Downlink (DL) transmission in a HetNet with J BSs and K single-antenna users is considered. We let $j \in \mathcal{B} = \{1, 2, \dots, J\}$ and $k \in \mathcal{U} = \{1, 2, \dots, K\}$ be the index of BSs and users, respectively. The number of antennas at BS j is denoted by M_j with $M_j \gg 1$. We assume time division duplex (TDD) operation with reciprocity-based CSI acquisition [4, 23]. Hence, each user sends a single uplink (UL) pilot to train *multiple nearby* BSs. In contrast to feedback-based CSI acquisition, this enables the training of large antenna arrays with overhead proportional to the number of simultaneously served users. Moreover, it enables CoMP with practical training overhead.

³Some of these results are also published in [38].

A. Channel Model

We denote the transpose and conjugate transpose of matrices by $(\cdot)^T$ and $(\cdot)^H$, respectively. We denote the transmit power of BS j by P_j . We assume a block-fading channel model where the channel coefficients remain constant within each RB [4, 5, 23, 39]. On a generic RB, we denote the channel matrix between BS j and users by \mathbf{G}_j , with the k^{th} column being $\mathbf{g}_{kj} = [g_{kj,1}, \dots, g_{kj,M_j}]^T$, where $g_{kj,i} = \sqrt{\beta_{kj}}h_{kj,i}$ is the channel between the i^{th} transmit antenna of BS j and user k , which includes both slow fading β_{kj} and fast fading $h_{kj,i}$. The slow fading β_{kj} characterizes the combined effect of distance-based path loss and location-based shadowing. We assume each link experiences independent Rayleigh fading, i.e., $\mathbf{h}_{kj} = [h_{kj,1}, \dots, h_{kj,M_j}]^T$ are complex Gaussian i.i.d. random variables. We let \mathbf{F}_j denote the precoding matrix at BS j , whose k^{th} column \mathbf{f}_{kj} is the beam (i.e., the precoding vector) for user k . The signal symbol of user k is denoted by s_k , where s_k has unit energy. The thermal noise at user k is denoted by w_k , which is assumed to be additive white Gaussian noise (AWGN) with variance σ^2 .

B. Admissible Joint Transmission

With massive MIMO, a subset of users are scheduled on each RB. In particular, the coded data for any given user can be transmitted either from a single BS – called *cellular transmission*, or from multiple BSs via CoMP. General CoMP poses many challenges making the extension from cellular transmission nontrivial. Key challenges include additional overhead for CSI exchanges among cooperating BSs, users' various preferences to different clusters, and the dependence of a user's rate on the other users served by the same BS. To address these challenges, we consider the following particular form of CoMP which can cover the formulation including various techniques (cellular, JT, blanking) as special cases. We denote by S_j the number of users that can be simultaneously served by BS j in the cellular transmission.

Definition 1. Admissible Transmission Schemes (ATs): An ATs schedules users for transmission on a sequence of RBs, and satisfies the following on each RB:

- (1) All users served by a given BS j are served in clusters of the same size L , for some $L \geq 1$;
- (2) BS j in clusters of size L serves at most $S_j(L)$ users with $S_j \leq S_j(L) \leq LS_j$ and $M_j \gg S_j(L)$;
- (3) The user beams (i.e., precoding vectors) at BS j are designed as if BS j was in cellular multi-user (MU)-MIMO transmission over all the users it serves;
- (4) All BSs serving a user transmit the same coded data stream to the user. Each BS transmits the stream on a beam that is (independently) designed for the users at that BS.

TABLE I
EXAMPLE OF RBs ENABLED BY ADMISSIBLE JT OVER 4 BSs.

RB		BS 1	BS 2	BS 3	BS 4
	Cluster Size	1	1	1	1
#1	User Power	1/2	1/2	1/2	1/2
	Served Users	1,2	3,4	5,6	7,8
	Cluster Size	2	2	2	2
#2	User Power	1/3	1/3	1/3	1/3
	Served Users	1,2,3	1,2,3	4,5,6	4,5,6
	Cluster Size	2	2	2	2
#3	User Power	1/3	1/3	1/3	1/3
	Served Users	1,2,3	1,4,5	2,4,6	3,5,6
	Cluster Size	2	2	1	1
#4	User Power	1/3	1/3	1/2	1/2
	Served Users	1,2,3	1,2,3	4,5	6,7

We assume each BS equally allocates its power to the set of scheduled users. The corresponding spectral efficiency can be viewed as a lower bound for cases with power optimization. To make it concrete, we give an ATS example in Table I, involving clusters of size 1 (i.e., cellular transmission) and 2. Four BSs are considered with $P_j = 1$, $S_j(1) = 2$ and $S_j(2) = 3$. As the table reveals, each BS on RB #1 engages in cellular transmission. On RB #2, pairs of BSs perform JT with each BS pair serving a triplet of users. RBs #3 and #4 provide additional more interesting modes. On RB #3, no user is served by the same cluster. On RB #4, BSs 1 and 2 serve users in clusters of size 2, while BSs 3 and 4 serve users in cellular transmission. Note that if orthogonal pilots are used, (at least) 8, 6, 6 and 7 uplink pilot dimensions (one dimension per user) are needed to enable RBs #1, #2, #3 and #4, respectively. Evidently, the choice of scheduled user sizes $S_j(L)$ signifies how aggressively pilot dimensions are reused across the network (e.g., S_j for fully reused pilots and LS_j for orthogonal pilots).

It is worth making a few remarks regarding the choice of ATSS in Defn. 1. First, the schemes of Defn. 1 provide the following CoMP benefits:

(1) **Performance gain at the cell edge:** The BF gain becomes intra-cluster BF gain in JT, as the same coded data is transmitted from all BSs serving the user. Similarly, the intra-cell interference mitigation is extended across the cluster of BSs by which the user is served. As a result, the performance gain can be realized at the cell edge.

(2) **Low training overhead:** An UL pilot from a user can be received at all nearby BS antennas, whether these are in the same or different locations. Thus, the CSI acquisition between a user and nearby BSs need not incur additional overhead with respect to cellular transmission in the TDD system.

(3) **BSs in JT may serve more users simultaneously than in cellular transmission:** Recall that the service capability (i.e., the number of simultaneously served users) of BS j in clusters of size L , $S_j(L)$, essentially depends on the number of available UL pilot resources. Thus, BSs in clusters may serve more users than in cellular transmission if UL pilots are not fully reused. For example, in Table I with orthogonal pilots, each BS can serve 2 UEs on RB #1 requiring 8 UL pilots, while each BS can serve 3 UEs on RB #2 requiring only 6 UL pilots. This implies that BSs may serve more users at each RB in JT versus the cellular transmission, but the power allocated from each BS to each user is reduced.

In addition, ATs possess several important properties that are not present in general CoMP schemes:

(a) **Local precoding at each BS:** This is due to (iii) in Defn. 1. For instance, the beam with Linear Zeroforcing Beamforming (LZFBF) for each user served by BS j is chosen within the null space of the channels of all the other users served by BS j , no matter whether there are additional BSs serving the user on the same RB or not.

(b) **No need for CSI exchange among BSs:** Due to local precoding, BS j only needs CSI between the users it serves and its own antennas to generate the user beams. In contrast to general CoMPs [18, 40, 41] that design beams depending on CSI between *other users* and *all BSs* in the cluster and thus require global CSI, the proposed JT only requires local CSI and does not introduce additional overhead.

(c) **Predictable instantaneous rates:** As shown in [41], the instantaneous user rates can also be predicted *a priori* with CoMP. However, unlike the general CoMP schemes, where a user's instantaneous rate depends on the other users scheduled on the same RB [41], the instantaneous rate in the ATs is *independent* of the other users channels in the scheduling set.

(d) **Flexible scheduling with user-specific clusters:** Revoking the local precoding again, each BS only needs to know which subset of users to serve on each RB. This allows users to be served by overlapping but different BS clusters on the same RBs (see, e.g., RB #3 in Table I).

Besides the flexibility in the cluster choices on each RB, in HetNets, we have another dimension of flexibility – the operation choices: an RB may have different subsets of BSs transmitting, depending on how network resources are shared between different layers. On some frequency band (a group of RBs) macro and small cell layers may operate together, while on some other band it might be only the macro layer operating or the small cell layer operating. We call these 3 different operations as *shared*, *macro-only* and *blanking operations*, respectively. Let $A \in \{1, 2, 3\}$ denote the operation type, where $A = 1$, $A = 2$ and $A = 3$ denote shared, macro-only and blanking operations, respectively. Let

RBs allocated to operation A form Band- A , and the set of BSs that can transmit in Band- A be $\mathcal{B}^{(A)}$.

Denoting by \mathcal{B}_m and \mathcal{B}_s the set of macro and small BSs, respectively, we have the following cases:

- 1) $A = 1$: shared operation is considered for this band, where macro and small cell BSs can both transmit, i.e., $\mathcal{B}^{(1)} = \mathcal{B}$. In this band, clusters can be formed by BSs from different layers.
- 2) $A = 2$: macro-only operation is considered for this band, and only macros can transmit, i.e., $\mathcal{B}^{(2)} = \mathcal{B}_m$.
- 3) $A = 3$: blanking operation is applied to this band, where macro BSs are muted, i.e., $\mathcal{B}^{(3)} = \mathcal{B}_s$.

Different resource allocations among operations refer to different scenarios. For example, scenarios with $A \in \{2, 3\}$ correspond to cases where orthogonal RBs are allocated to macro and small cells, while scenarios with $A \in \{1, 3\}$ can be applied to cases with eICIC. In some scenarios, resource allocation among operations can be fixed *a priori*. In more flexible scenarios, resource allocation among operations can be a part of the optimization problem. Our formulation in Sec. IV can be applied to both cases.

To show how these different transmission operations of practical interest can be considered within ATSS, we give a small example in Table II. As different bands may prefer different cluster sizes, we consider clusters up to size $L_{\max}^{(A)}$ in Band- A , where clusters of size $L \leq L_{\max}^{(A)}$ in this band is determined by the subsets of $\mathcal{B}^{(A)}$ with size less than or equal to $L_{\max}^{(A)}$ ⁴. Table II is extended from Table I by adding the macro BS (BS #5) and considering other BSs as small cell BSs, i.e., $\mathcal{B}_m = \{5\}$ and $\mathcal{B}_s = \{1, 2, 3, 4\}$. In this example, we let $L_{\max}^{(1)} = 2$, $L_{\max}^{(2)} = 1$ and $L_{\max}^{(3)} = 2$. RBs b and d are in Band-1, RB e is in Band-2, and RBs a and c are in Band-3. RBs b and d represent shared operation. In RB b , each BS is doing cellular transmission. On the other hand, RB d considers clusters of size 2, which include both macro and small cell BSs. RB e represents macro only operation, where the macro BS (BS #5) is serving users 1 and 2 by cellular transmission. In RBs a and c , blanking is applied, i.e. only small cells serve users while macro BS is muted. Hence, clusters do not include macro BSs. In fact, the clusters in RBs a and c are the same as in RB #1 and RB #3 in Table I, respectively.

III. INSTANTANEOUS RATE AND LONG-TERM RATE

In this section, we provide proxy expressions for instantaneous rates and long-term rates (throughput) with either LZFBF or Maximum Ratio Transmission (MRT, also known as Conjugate Beamforming).

We consider a scheduling policy on RBs $\{1, 2, \dots, T\}$ and assume that all the large-scale coefficients stay fixed within this period. Any such scheduling policy can be described in terms of the scheduling

⁴Many of these clusters are not necessary. For example clusters between BSs that are geographically distant are not necessary to consider as users should not be assigned to these clusters. This type of practical observations can eliminate many cluster options for all RBs.

TABLE II
EXAMPLE OF RBs ENABLED BY ADMISSIBLE JT OVER 4 SMALL CELL BSs (BSs 1-4) AND 1 MACRO BS (BS 5).

RB		BS 1	BS 2	BS 3	BS 4	(Macro) BS 5
	Cluster Size	1	1	1	1	-
a	User Power	1/2	1/2	1/2	1/2	-
	Served Users	1,2	3,4	5,6	7,8	-
	Cluster Size	1	1	1	1	1
b	User Power	1/2	1/2	1/2	1/2	1/2
	Served Users	1,2	3,4	5,6	7,8	9,10
	Cluster Size	2	2	2	2	-
c	User Power	1/3	1/3	1/3	1/3	-
	Served Users	1,2,3	1,4,5	2,4,6	3,5,6	-
	Cluster Size	2	2	2	2	2
d	User Power	1/3	1/3	1/3	1/2	1/3
	Served Users	1,2,3	1,4,5	2,4,6	3,7	5,6,7
	Cluster Size	-	-	-	-	1
e	User Power	-	-	-	-	1/2
	Served Users	-	-	-	-	1,2

sets $\{\mathcal{U}_c(t); \forall \mathcal{C}, \forall t \in \{1, 2, \dots, T\}\}$, where $\mathcal{U}_c(t)$ denotes the set of users served by cluster \mathcal{C} on RB t . Without loss of generality, we assume that RB t is in Band- A and user k is served by the cluster $\mathcal{C} \subset \mathcal{B}^{(A)}$ on RB t . Thus, the received signal at user $k \in \mathcal{U}_c(t)$ on RB t can be expressed by

$$\begin{aligned}
 y_k(t) = & \underbrace{\sum_{j \in \mathcal{C}} \sqrt{\frac{P_j}{S_j(|\mathcal{C}|)}} \mathbf{g}_{kj}(t)^H \mathbf{f}_{kj}(t) s_k}_{\text{desired}} + \underbrace{\sum_{j \in \mathcal{C}} \sum_{u \in \mathcal{U}_c(t), u \neq k} \sqrt{\frac{P_j}{S_j(|\mathcal{C}|)}} \mathbf{g}_{kj}(t)^H \mathbf{f}_{uj}(t) s_u}_{\text{intra-cluster interference}} \\
 & + \underbrace{\sum_{l \notin \mathcal{C}} \sum_{u \in \cup_{\mathcal{C}' : l \in \mathcal{C}'} \mathcal{U}_{\mathcal{C}'}(t)} \sqrt{\frac{P_l}{S_l(|\mathcal{C}'|)}} \mathbf{g}_{kl}(t)^H \mathbf{f}_{ul}(t) s_u}_{\text{inter-cluster interference}} + \underbrace{w_k}_{\text{noise}}. \tag{1}
 \end{aligned}$$

Adopting LZFBF, the precoding matrix at BS j is $\mathbf{F}_j = \mathbf{G}_j (\mathbf{G}_j^H \mathbf{G}_j)^{-1} \mathbf{A}_j^{1/2}$, where \mathbf{A}_j is the normalizing coefficients matrix. In this case, the intra-cluster interference is 0. With MRT, the precoding matrix at BS j is \mathbf{F}_j with the k th column being $\mathbf{f}_{kj} = \frac{\mathbf{g}_{kj}}{\|\mathbf{g}_{kj}\|}$. Note that the set of interfering BSs depends on the operation band.

A. Instantaneous Rate

In this paper, we assume that each BS has perfect CSI. Consider cellular transmission, let S_j denote the number of users served by BS j on a given RB, with $S_j \ll M_j$. Under mild assumptions on fading, the achievable user instantaneous rates on RB t , $r_{kj}(t)$, can be predicted *a priori* in the massive MIMO regime [15]. In particular, there exist deterministic quantities $\{r_{kj}\}$ such that $r_{kj}(t) \xrightarrow{\text{a.s.}} r_{kj}, \forall k \in \mathcal{U}$ and

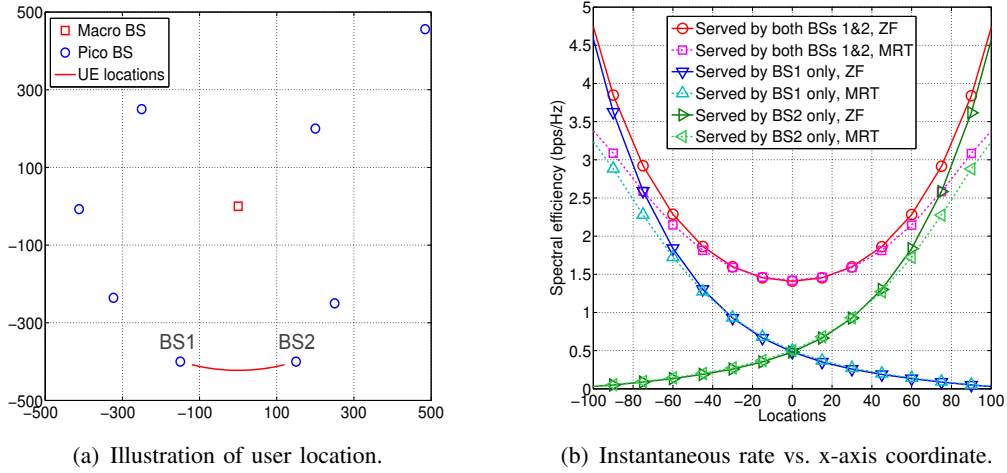


Fig. 1. Illustration of instantaneous rate versus user locations, when $S_j(|\mathcal{C}|) = |\mathcal{C}|S_j$. The location in Fig. 1(b) indicates the x-axis coordinate of the path in Fig. 1(a). The cell edge users (e.g., the areas near the origin) benefit from joint transmission.

$\forall j \in \mathcal{B}$, as $M_j, S_j \rightarrow \infty$, with fixed $v_j = S_j/M_j \geq 0$ [4, 5, 23]. This convergence is very fast with respect to M_j 's. As shown in [41], the instantaneous user rates can also be predicted *a priori* with CoMP. However, unlike general CoMP settings, where a user's instantaneous rate depends on the other users co-scheduled for transmission on the same RB [41], the schemes of Defn. 1 make a user's instantaneous rate *independent* of the identities of the other users in the scheduling set.

Let $r_{k\mathcal{C}}(t)$ be the instantaneous rate of user k from cluster \mathcal{C} on RB t in Band- A . There exist deterministic quantities $\{r_{k\mathcal{C}}^{(A)}\}$ such that $r_{k\mathcal{C}}(t) \xrightarrow{\text{a.s.}} r_{k\mathcal{C}}^{(A)}$, for RB- t in Band- A for all $k \in \mathcal{U}$, $\mathcal{C} \subset \mathcal{B}(A)$ and $A \in \{1, 2, 3\}$, as $M_j, S_j(|\mathcal{C}|) \rightarrow \infty$ with fixed $v_j = S_j(|\mathcal{C}|)/M_j \geq 0$ for all $j \in \mathcal{C}$.

Using the techniques in [41, 42], we can show that the approximate instantaneous rate of user k from cluster $\mathcal{C} \subset \mathcal{B}^{(A)}$ in Band- A using LZFBF is

$$r_{k\mathcal{C}}^{(A)} = \log_2 \left(1 + \frac{\sum_{j \in \mathcal{C}} \sum_{l \in \mathcal{C}} \sqrt{P_j P_l \beta_{kj} \beta_{kl} b_j(|\mathcal{C}|) b_l(|\mathcal{C}|)}}{\sigma^2 + \sum_{l \notin \mathcal{C}, l \in \mathcal{B}^{(A)}} P_l \beta_{kl}} \right), \quad (2)$$

where $b_j(a) = \frac{M_j - S_j(a) + 1}{S_j(a)}$. Similarly, the approximate instantaneous rate of user k from cluster \mathcal{C} in Band- A using MRT is

$$r_{k\mathcal{C}}^{(A)} = \log_2 \left(1 + \frac{\sum_{j \in \mathcal{C}} \sum_{l \in \mathcal{C}} \sqrt{\frac{P_j P_l M_j M_l \beta_{kj} \beta_{kl}}{S_j(|\mathcal{C}|) S_l(|\mathcal{C}|)}}}{\sigma^2 + I_{k\mathcal{C}} + \sum_{l \notin \mathcal{C}, l \in \mathcal{B}^{(A)}} P_l \beta_{kl}} \right), \quad (3)$$

where $I_{k\mathcal{C}} = \sum_{j \in \mathcal{C}} \frac{(S_j(|\mathcal{C}|) - 1)}{S_j(|\mathcal{C}|)} P_j \beta_{kj}$ is the non-zero intra-cluster interference. Clearly, $r_{k\mathcal{C}}^{(A)} = 0$ if $\mathcal{C} \not\subset \mathcal{B}^{(A)}$.

Eqs. (2) and (3) assume that $\forall j \in \mathcal{C}$, BS j serves $S_j(|\mathcal{C}|)$ users and allocates $P_j/S_j(|\mathcal{C}|)$ fraction of its power to each user. In the case that fewer users are served by one of the BSs, (2) and (3) represent achievable lower-bound instantaneous rates.

Recalling that macro BSs do not transmit in Band-3 (i.e., the blanking operation), the instantaneous

rate from macro BSs to users in this band is therefore 0, while there is no interference from macro BSs to small cell users. Obviously, the users in small cells would benefit from larger SINR in Band-3.

For JT, we give an illustration example in Fig. 1 to show the change of instantaneous rate versus user locations. When the user is close to the origin, which is the cell edge area of BSs 1 and 2, the instantaneous rate from cluster $\{1, 2\}$ is about $3\times$ compared to the case where users are served by an individual BS. This implies the potential benefits of JT for cell-edge users.

B. Long-term Rate

As discussed in Sec. I-A, the user association and scheduling problems are generally coupled with each other. On the other hand, as shown in (2) and (3), the instantaneous rate with massive MIMO does not depend on the fast fading and user scheduling. Moreover, the UL pilots can be received at all nearby BSs, and thus users can be served by different BSs on different RBs [15]. Therefore, users can be served (at different times) by more than one BS unlike the conventional approach. Similarly in JT with Massive MIMO, users can be served by different clusters on different RBs. The long term rate a user gets is a combination of all the rates it gets from different clusters. This simplifies the coupled relationship between user association and scheduling, exploiting which we can relax the requirement of *a priori* knowledge of available resources per user given the association (e.g., the equal resource allocation in [9, 14]), and jointly optimize the user association and its corresponding scheduling as studied in [15].

Let $x_{k\mathcal{C}}^{(A)} = \lim_{T \rightarrow \infty} \frac{|\{t: 1 \leq t \leq T, k \in \mathcal{U}_{\mathcal{C}}^{(A)}(t), t \text{ in Band-}A\}|}{T}$ be the fraction of resources allocated by cluster \mathcal{C} to user k in Band- A – called *activity fraction*. If $x_{k\mathcal{C}}^{(A)} > 0$, user k is served by cluster \mathcal{C} in Band- A . We obtain the long-term rate similar to [15], which depends on instantaneous rates and activity fractions from the scheduling policy. In the limit $T \rightarrow \infty$, the long-term rate of user k can be expressed by⁵

$$R_k = \sum_{A=1}^3 \sum_{\substack{\mathcal{C}: \mathcal{C} \subset \mathcal{B}^{(A)} \\ |\mathcal{C}| \leq L_{\max}^{(A)}}} x_{k\mathcal{C}}^{(A)} r_{k\mathcal{C}}^{(A)}. \quad (4)$$

IV. UNIFIED NUM PROBLEM FORMULATION

While the ATS definition allows for varying cluster sizes within an RB as revealed in Table I, for practical interest and tractability, in the sequel we specialize to the case with equal-size clusters on each RB. Consequently, the following framework allows for cluster options as seen in RBs #1-3 but not for RB #4 in Table I. We call this new scheme the Uniform Cluster-Size scheme (UCS).

⁵Convergence to the limiting expressions of interest is very quick [15].

Definition 2. Uniform Cluster-Size Scheme (UCS): An ATS from Defn. 1 is a UCS if

- (1) μ_A fraction of RBs is allocated to Band- A , with $\sum_A \mu_A \leq 1$;
- (2) For each Band- A , λ_{AL} fraction of RBs is allocated to size- L clusters for $1 \leq L \leq L_{\max}^{(A)}$, with $\sum_{L=1}^{L_{\max}^{(A)}} \lambda_{AL} \leq \mu_A$;
- (3) on any RB in the λ_{AL} fraction, the scheduled users are served by (user-dependent) clusters of the same size L and these clusters are formed by BSs in $\mathcal{B}^{(A)}$;
- (4) on any RB in the λ_{AL} fraction, each BS does not serve more than $S_j(L)$ users.

Then ATS designs considered in the rest of the paper are all *Uniform Cluster-Size Scheme*. RBs allocated to serving size- L clusters in Band- A is called the L^{th} subband of Band- A . The NUM problem for the UCS optimizes activity fractions and subband/band allocations is given as follows:

$$\max_{\lambda_{AL}, x_{kC}^{(A)}, \mu_A} \sum_{k \in \mathcal{U}} U \left(\sum_{A=1}^3 \sum_{\substack{C: C \subset \mathcal{B}^{(A)}, \\ |C| \leq L_{\max}^{(A)}}} x_{kC}^{(A)} r_{kC}^{(A)} \right) \quad (5a)$$

$$\text{s.t.} \quad \sum_{\substack{C: C \subset \mathcal{B}^{(A)}, \\ j \in C, |C|=L}} \frac{\sum_{k \in \mathcal{U}} x_{kC}^{(A)}}{S_j(L)} \leq \lambda_{AL}, \quad \forall j \in \mathcal{B}^{(A)}, \forall L \leq L_{\max}^{(A)}, \forall A, \quad (5b)$$

$$\sum_{C: |C|=L, C \subset \mathcal{B}^{(A)}} x_{kC}^{(A)} \leq \lambda_{AL}, \quad \forall k \in \mathcal{U}, \forall L \leq L_{\max}^{(A)}, \forall A, \quad (5c)$$

$$\sum_{L=1}^{L_{\max}^{(A)}} \lambda_{AL} \leq \mu_A, \quad \forall A, \quad (5d)$$

$$\sum_{A=1}^3 \mu_A \leq 1, \quad (5e)$$

$$x_{kC}^{(A)}, \lambda_{AL}, \mu_A \geq 0, \quad \forall k \in \mathcal{U}, \forall C, \forall L \leq L_{\max}^{(A)}, \forall A, \quad (5f)$$

where the utility function $U(\cdot)$ is a continuously differentiable, monotonically increasing, and strictly concave function [43]. Constraint (5b) signifies that the total activity fractions allocated by BS j in clusters of size L in Band- A cannot exceed the total available resources $\lambda_{AL} S_j(L)$. On the other hand, recalling that each user cannot be served by multiple clusters on the same RBs, (5c) signifies that the fraction of RBs over which user k is served by clusters of size L in Band- A cannot exceed RBs allocated to the clusters of size L in Band- A , λ_{AL} . (5d) ensures that the total resources allocated to the subbands in Band- A are no more than the resources allocated to that band. Finally, (5e) signifies the fact that the summation of resources allocated to different bands is equal to all available resources.

Remark 1. The formulation (5) is quite flexible. It can be applied to not only the scenarios that optimize the resource allocation among operations, but also the scenarios where resources given to each operation is fixed a priori by setting corresponding μ_A variables to constants in (5).

Remark 2. The NUM problem of [15] can be obtained a special case of 5) by setting $A = 1$ and $L_{\max}(1) = 1$.

In this paper, we specify the utility in (5) to the logarithmic utility as [14, 15, 29]. Logarithmic function as a very common choice of utility function, is well known for striking good balance between network throughput and user fairness [44]. It is easy to verify that (5) is a convex optimization problem [45]. General numerical solvers (e.g., CVX) can be used. Since CVX is not well-suited for large instances [46], we alternatively propose an efficient algorithm that can be applied to large networks in the next section.

V. DUAL SUBGRADIENT BASED ALGORITHM

In this section, we propose an efficient algorithm based on the dual subgradient method [45]. We let $\nu_{jL}^{(A)}$ and $\theta_{kL}^{(A)}$ be the Lagrange multipliers corresponding to (5b) and (5c), respectively. The dual problem of (5) is

$$\min_{\nu_{jL}^{(A)}, \theta_{kL}^{(A)} \geq 0} \sum_{k \in \mathcal{U}} f_k \left(\nu_{jL}^{(A)}, \theta_{kL}^{(A)} \right) + g \left(\nu_{jL}^{(A)}, \theta_{kL}^{(A)} \right),$$

where

$$\begin{aligned} f_k \left(\nu_{jL}^{(A)}, \theta_{kL}^{(A)} \right) = \max_{x_{kC}^{(A)} \geq 0} \log & \left(\sum_{A=1}^3 \sum_{\substack{C: C \subset \mathcal{B}^{(A)}, \\ |C| \leq L_{\max}^{(A)}}} x_{kC}^{(A)} r_{kC}^{(A)} \right) - \sum_{A=1}^3 \sum_{L=1}^{L_{\max}^{(A)}} \sum_{\substack{C: C \subset \mathcal{B}^{(A)}, \\ |C|=L}} \sum_{j: j \in C} \frac{\nu_{jL}^{(A)}}{S_j(L)} x_{kC}^{(A)} \\ & - \sum_{A=1}^3 \sum_{L=1}^{L_{\max}^{(A)}} \theta_{kL}^{(A)} \sum_{C: C \subset \mathcal{B}^{(A)}, |C|=L} x_{kC}^{(A)}, \end{aligned} \quad (6)$$

and

$$g \left(\nu_{jL}^{(A)}, \theta_{kL}^{(A)} \right) = \max_{\substack{\sum_{L=1}^{L_{\max}^{(A)}} \lambda_{AL} \leq \mu_A, \\ \sum_{A=1}^3 \mu_A \leq 1}} \sum_{A=1}^3 \sum_{L=1}^{L_{\max}^{(A)}} \left(\sum_{j: j \in \mathcal{B}^{(A)}} \nu_{jL}^{(A)} + \sum_{k \in \mathcal{U}} \theta_{kL}^{(A)} \right) \lambda_{AL}. \quad (7)$$

The constraints of (5) satisfy the Slater condition [45], and thus strong duality holds (i.e., the dual problem and the original problem (5) have the same optimal value).

A. The Dual Subgradient Method

The optimization problem (6) has the closed-form optimal solution

$$x_{kC}^{(A)} = \begin{cases} \frac{1}{\sum_{L:L=|C|} \left(\sum_{j:j \in C} \nu_{jL}^{(A)} / S_j(L) + \theta_{kL}^{(A)} \right)}, & \text{if } \{C, A\} = \{C^*, A^*\}, \\ 0, & \text{otherwise,} \end{cases} \quad (8)$$

where $\{C^*, A^*\} = \arg \max_{C, A} \frac{r_{kC}^{(A)}}{\sum_{L:L=|C|} \left(\sum_{j:j \in C} \nu_{jL}^{(A)} / S_j(L) + \theta_{kL}^{(A)} \right)}$ ⁶.

The problem (7) is a LP and one optimal solution is⁷

$$\lambda_{AL} = \begin{cases} 1, & \text{if } \{A, L\} = \arg \max_{A', L'} \sum_{j:j \in \mathcal{B}(A')} \nu_{jL'}^{(A')} + \sum_{k \in \mathcal{U}} \theta_{kL'}^{(A')}, \\ 0, & \text{otherwise,} \end{cases} \quad (9)$$

and

$$\mu_A = \begin{cases} 1, & \text{if there exists a band } A \text{ such that the above } \lambda_{AL} > 0, \\ 0, & \text{otherwise.} \end{cases} \quad (10)$$

The t th iteration of the algorithm is as follows.

- 1) Update the activity fractions by (8).
- 2) Update resource allocation for different bands and clusters by (9) and (10).
- 3) Update the Lagrangian multipliers by

$$\nu_{jL}^{(A)}(n+1) = \left[\nu_{jL}^{(A)}(n) - \delta(n) \left(\lambda_{AL}(n) - \sum_{\substack{C: C \subset \mathcal{B}(A), \\ j \in C, |C|=L}} \frac{\sum_{k \in \mathcal{U}} x_{kC}^{(A)}(n)}{S_j(L)} \right) \right]^+, \quad (11)$$

and

$$\theta_{kL}^{(A)}(n+1) = \theta_{kL}^{(A)}(n) - \delta(n) \left(\lambda_{AL}(n) - \sum_{C: C \subset \mathcal{B}(A), |C|=L} x_{kC}^{(A)} \right), \quad (12)$$

where $[z]^+ = \max\{z, 0\}$ and $\delta(n)$ is the stepsize at the n^{th} iteration.

By adding redundant constraints $x_{kC}^{(A)} \leq 1$ and choosing an appropriate stepsize (e.g, a diminishing stepsize $\delta(n) = \frac{a}{n+b}$, where a and b are some positive scalars), the subgradients can be bounded. This allows us leveraging Prop. 6.3.4. in [45] to show the convergence of the dual subgradient algorithm. For simplicity, we give the above key steps without introducing the redundant constraints. It is easy to extend the above algorithm to the cases with redundant constraints.

⁶If we have multiple pairs of $\{C^*, A^*\}$, we just randomly pick one pair.

⁷If we have multiple $\{A, L\}$ pairs that maximize the $\sum_{j:j \in \mathcal{B}(A)} \nu_{jL}^{(A)} + \sum_{k \in \mathcal{U}} \theta_{kL}^{(A)}$, we just randomly pick one.

B. Finding the Optimal Primal Solutions Given the Optimal Dual Variables

Note that the objective function of (5) is not strictly convex and we may have multiple optimal solutions. In this case, given the optimal dual variables, it is generally difficult to find the optimal primal solutions that satisfy the KKT conditions. However, by exploring the structure of (5) as follows, we propose to obtain the optimal primal solutions by solving a small-size LP.

The optimal long-term rate $R_k^* = \sum_{A=1}^3 \sum_{\mathcal{C}: \mathcal{C} \subset \mathcal{B}^{(A)}} x_{k\mathcal{C}}^{*(A)} r_{k\mathcal{C}}^{(A)}$ in (5) is unique, since the function $\log(R_k)$ is strictly concave with respect to R_k . KKT conditions of problem (5) imply

$$R_k \geq \frac{r_{k\mathcal{C}}^{(A)}}{\sum_{j:j \in \mathcal{C}} \nu_{j|\mathcal{C}}^{(A)} / S_j(|\mathcal{C}|) + \theta_{k|\mathcal{C}}^{(A)}}. \quad (13)$$

Thus, given the optimal dual variables, the unique optimal rate can be easily obtained by $R_k^* = \max_{\mathcal{C}, A} \left\{ \frac{r_{k\mathcal{C}}^{(A)}}{\sum_{j:j \in \mathcal{C}} \nu_{j|\mathcal{C}}^{(A)} / S_j(|\mathcal{C}|) + \theta_{k|\mathcal{C}}^{(A)}} \right\}$. We observe from (13) that in the optimal solutions, each user only has positive activity fractions $x_{k\mathcal{C}}^{(A)}$ to clusters providing the maximum term of the right-hand side of (13). Based on this conclusion, we propose the following LP, whose size is reduced by only focusing on the positive $x_{k\mathcal{C}}^{(A)}$ obtained from (13).

$$\begin{aligned} & \max_{\eta, x, \lambda} \eta \\ & \text{s.t. } \eta \leq \sum_{A=1}^3 \sum_{\mathcal{C} \subset \mathcal{B}^{(A)}} \frac{x_{k\mathcal{C}}^{(A)} r_{k\mathcal{C}}^{(A)}}{R_k^*}, \quad \forall k \in \mathcal{U}, \\ & (5b) - (5f). \end{aligned} \quad (14)$$

Proposition 1. *Given that R_k^* is the exact optimal rate of (5), the solution of (14) are the same as the optimal solutions of problem (5).*

Proof: Similar techniques in the proof of Lemma 1 in [15] can be used to complete this proof. ■

Prop. 1 implies that we can obtain the solutions of (5) given the optimal dual variables. Though we can show the convergence of the dual subgradient algorithm by adding redundant constraints, there may exist a small gap between the obtained dual variables and the optimal ones, due to the numerical precision or the limit on the number of iterations. Exploiting the well-behaved structure of (14), i.e., finite coefficients and a bounded feasible set [15], it is expected that the solution of (14) is near optimal in the presence of a small gap between the obtained dual variables and the optimal ones.

Empirical evidence reveals that in a heavily loaded network, where constraints (5c) are inactive (i.e., $\sum_{\substack{\mathcal{C}: |\mathcal{C}|=L, \\ \mathcal{C} \subset \mathcal{B}^{(A)}}} x_{k\mathcal{C}}^{(A)} < \lambda_{AL}$), most users are uniquely served by one cluster on each subband. Insight regarding this observation can be obtained by examining KKT conditions of (5).

Proposition 2. For a given Band-A and a cluster size L , if (5c) are inactive $\forall k \in \mathcal{U}$, the number of users that are served by multiple BS clusters on RBs allocated to L^{th} subband of Band-A is at most $N_{CL}^{(A)} - 1$, where $N_{CL}^{(A)}$ is the number of clusters in the L^{th} subband of Band-A.

Proof: See Appendix B. ■

Prop. 2 implies that the optimal user associations in each subband are mostly unique. We call the users served by more than one cluster on any subband as “fractional users”. Note that Prop. 2 provides an upper bound (i.e., $N_{CL}^{(A)}$) on the number of fractional users, while simulations show a much smaller number of fractional users than $N_{CL}^{(A)}$ (less than 3.5% K in Sec. VII). Recall that the dual subgradient algorithm determines the set of positive activity fractions, i.e., $x_{kC}^{(A)}$ of users to their cluster-band pairs $\{C^*, A^*\}$, while the rest of activity fractions are zero. Thus, the unknown activity fractions that needs to be solved via (14) are only the positive activity fractions. Based on Prop. 2, most users (with unique association) have at most one positive activity fraction on any subband. Thus, the size of (14) is significantly reduced, implying the efficiency of the proposed algorithm. Further details regarding the algorithm complexity can be found in Appendix C.

As a result, we propose an efficient algorithm that can be applied to large network instances. Unlike the cellular case investigated in [15], it is not *a priori* known whether the optimal NUM solution can be implemented via any scheduler or not. The implementation of NUM solutions is discussed below.

VI. SCHEDULING

In this section, we aim to propose scheduling policies that yield activity fractions closely matching the NUM solution. Each band conducts scheduling independently. Considering a scheduling policy for Band-A and letting $L(t)$ be the cluster size in RB t , we define the feasible scheduling policy as follows.

Definition 3. Feasible Schedule: A scheduling policy $\{\mathcal{U}_C(t); , \forall C \subset \mathcal{B}^{(A)}, |C| \leq L_{\max}^{(A)}, \forall t \text{ in Band-A}\}$ is feasible with respect to the UCS based on Defn. 2, if it satisfies the following:

- (i) For each t , the policy assigns RB t to clusters with $C \subset \mathcal{B}^{(A)}$ and $|C| = L(t)$ in Band-A; that is, for each cluster C with $\mathcal{U}_C(t)$ being non-empty, we have $C \subset \mathcal{B}^{(A)}$ and $|C| = L(t)$.
- (ii) For each t , each user is served by at most one cluster; that is, $|\sum_{C \subset \mathcal{B}^{(A)}} \mathbb{1}\{k \in \mathcal{U}_C(t)\}| \leq 1$.
- (iii) For each t in Band-A and for each BS $j \in \mathcal{B}^{(A)}$, BS j serves at most $S_j(L(t))$ users; that is, $|\cup_{C: j \in C, C \subset \mathcal{B}^{(A)}} \mathcal{U}_C(t)| \leq S_j(L(t))$.

A. The Feasibility of the NUM Solution in Implementation

It is easy to verify that $\{x_{kC}^{(A)}\}$ yielded by any feasible schedules defined by Defn. 3 satisfy (5b)–(5f). In fact, when $L_{\max}^{(A)} = 1$ (i.e., cellular cases), there exists at least one feasible schedule for Band- A that can provide long-term activity fractions approaching the solution of (5) as shown in [15]. However, for networks with cluster combinations $\{j_1, j_2\}$, $\{j_1, j_3\}$ and $\{j_2, j_3\}$, where j_1, j_2 and j_3 are BS indexes, there exist $\{x_{kC}^{(A)}\}$ satisfying (5b)–(5f), for which no feasible schedule of Defn. 3 exists.

Theorem 1. *In the UCSs with $L_{\max}^{(A)} > 1$ in some Band- A and with the type of cluster combinations $\{j_1, j_2\}$, $\{j_1, j_3\}$ and $\{j_2, j_3\}$, where j_1, j_2 and j_3 are BSs in $\mathcal{B}^{(A)}$, there exist some activity fractions satisfying (5b)–(5f) that cannot be implemented by any feasible schedule in Defn. 3.*

Proof: See Appendix A. ■

Hence, the coarser time-scale NUM problem (5) does not capture the finer time-scale constraints associated with feasible schedulers. Although, in general, (5) provides an upper bound on the network performance, as we show next, using activity fractions that are the solution to (5), we can design scheduling policies, whose performance is close to the utility provided by the solution to (5).

B. Virtual Queue Based Scheduling Scheme

We consider scheduling policies for the UCS architecture comprised of $\sum_{A=1}^3 L_{\max}^{(A)}$ parallel schedulers, one per each subband. We describe a method for scheduling users over the RBs from the $\lambda_{AL} > 0$ fraction of RBs dedicated to clusters of size L in band- A .

Given the limited number of fractional users per cluster size L , the scheduler approximates the optimal $\{x_{kC}^{(A)}\}$ by unique association activity fractions, $\{\tilde{x}_{kC}^{(A)}\}$, given by

$$\tilde{x}_{kC}^{(A)} = \begin{cases} x_{kC}^{(A)} & \text{if } \mathcal{C} = \mathcal{C}^*(k) \\ 0 & \text{otherwise} \end{cases}, \quad (15)$$

with $\mathcal{C}^*(k) = \arg \max_{\mathcal{C}: |\mathcal{C}|=L, \mathcal{C} \subset \mathcal{B}^{(A)}} x_{kC}^{(A)}$.

Letting $\mathcal{U}_{\mathcal{C}}^{(A)}$ denote the users for which $\tilde{x}_{kC}^{(A)} > 0$, we have $\mathcal{U}_{\mathcal{C}}^{(A)} \cap \mathcal{U}_{\mathcal{C}'}^{(A)} = \emptyset$ for all $\mathcal{C} \neq \mathcal{C}'$ with $|\mathcal{C}| = |\mathcal{C}'|$. We also let $\mathcal{U}^{(AL)} = \cup_{\mathcal{C}: |\mathcal{C}|=L} \mathcal{U}_{\mathcal{C}}^{(A)}$ denote the set of users that receive non-zero activity fractions from clusters of size L in Band- A . In the rest of this section, we focus on clusters \mathcal{C} satisfying $|\mathcal{C}| = L$ and $\mathcal{C} \in \mathcal{B}^{(A)}$, unless otherwise specified.

To assign user k a fraction of RBs close to the desired fraction in the L^{th} subband of Band- A , i.e., $\alpha_k = \tilde{x}_{k\mathcal{C}^*(k)}^{(A)} / \lambda_{AL}$, we consider a max-min scheduling policy based on virtual queues (VQ), which

assumes user k receives rate $\tilde{R}_k = 1/\alpha_k$ when user k is scheduled for transmission by cluster $\mathcal{C}^*(k)$ (i.e., $k \in \mathcal{U}_{\mathcal{C}^*(k)}^{(A)}(t)$). The cluster-size L scheduler performs at each t a weighted sum rate maximization (WSRM) of the form [47]:

$$\max_{\tilde{\mathcal{U}} \subseteq \mathcal{U}^{(AL)}} \sum_{k \in \tilde{\mathcal{U}}} Q_k(t) \tilde{R}_k, \quad (16a)$$

$$\text{s.t.} \quad \sum_{k \in \tilde{\mathcal{U}}} \mathbb{1}\{j \in \mathcal{C}^*(k)\} \leq S_j(L), \quad \forall j \in \mathcal{B}, \quad (16b)$$

where the weight of user k at time t , $Q_k(t)$, is the VQ length of user k at time t . For max-min fairness [47], $Q_k(t)$ is updated as follows:

$$Q_k(t+1) = \max\{0, Q_k(t) - \tilde{R}_k(t)\} + A_k(t), \quad (16c)$$

where

$$\tilde{R}_k(t) = \begin{cases} \tilde{R}_k & \text{if user } k \text{ is scheduled at time } t \\ 0 & \text{otherwise} \end{cases}, \quad (16d)$$

$$A_k(t) = \begin{cases} A_{\max} & \text{if } V > \sum_k Q_k(t) \\ 0 & \text{otherwise} \end{cases}, \quad (16e)$$

with A_{\max} and V chosen sufficiently large [47]. Note that in the absence of constraints (16b), the max-min scheduler (16) schedules user k the desired fraction of RBs, α_k .

Scheduling via (16) is impractical, as it amounts to solving for each RB t an integer linear program of the form (16a)–(16b). A number of heuristic algorithms can be used to provide feasible (though generally suboptimal) solutions to (16). In this paper, we consider a rudimentary greedy algorithm. Letting $K_{AL} = |\mathcal{U}^{(AL)}|$ be the total number of users to be served by clusters of size L , the greedy algorithm for size- L clusters at time t operates as follows:

1. Determine a user order $\pi(k)$, where $Q_{\pi(k)}(t)\tilde{R}_{\pi(k)} \geq Q_{\pi(k+1)}(t)\tilde{R}_{\pi(k+1)}$ for all $k \in \mathcal{U}^{(AL)}$.
2. Initialization: $k = 1$, and $\tilde{\mathcal{U}} = \emptyset$.
3. If the user set $\tilde{\mathcal{U}} \cup \{\pi(k)\}$ satisfies all the constraints in (16b), set $\tilde{\mathcal{U}} = \tilde{\mathcal{U}} \cup \{\pi(k)\}$.
4. If $k < K_{AL}$, set $k = k + 1$ and go to step 3.
5. Output $\tilde{\mathcal{U}}$ as the scheduling user set for size- L clusters in Band- A at time t .

VII. PERFORMANCE EVALUATION

In this section, we present a simulation-based evaluation based on the “wrap-around” layout in Fig. 2. The parameters used are given as follows unless otherwise specified. There are 4 macros with $M_j = 100$ and $S_j(|C|) = \max\{10\rho|C|, 10\}$, and 32 pico BSs with $M_j = 40$ and $S_j(|C|) = \max\{4\rho|C|, 4\}$, with ρ being a tunable parameter in $[0, 1]$. There is 1 pico BS at the center of each white square, while 3 pico BSs being dropped uniformly within each shaded square (hotspot). Also, 15 and 90 single-antenna users are dropped uniformly in each white and shaded square, respectively. The macro and pico BS transmit powers are 46dBm and 35dBm, respectively. The path-loss for macro-user links and pico-user links are $128.1 + 37.6 \log_{10} d$ and $140.7 + 36.7 \log_{10} d$, respectively, with the distance d in km. The noise power spectral density is -174 dBm/Hz.

We consider three distinct macro-pico resource sharing scenarios: (i) the shared scenario with macros and picos transmitting on the same RBs – operations with $A = 1$; (ii) the orthogonal scenario with macros and picos transmitting on different bands – operations with $A \in \{2, 3\}$, where we provide macros (Band-2) 20% RBs as an illustrative example; (iii) RB blanking with macros muted on certain RBs – operations with $A \in \{1, 3\}$. Note that though we can jointly optimize the resource partition among different bands and user activity fractions using (5) in the orthogonal scenario, we fix $\mu_2 = 0.2$ and $\mu_3 = 0.8$. This is due to the fact that resource partition among macro and small cells is most likely static (or semi-static) in practice. Also, the macro and small cells may operate on different frequency bands (e.g., the macro BSs may transmit on lower-frequency bands, while the small cell BSs may transmit on higher-frequency bands), where μ depends on available bands and thus is not a variable to optimize.

We make comparisons between the conventional approach (denoted as max-SINR in the following), the approach of [15] and the proposed UCS of this work. Both max-SINR and [15] are cellular approaches. In fact the formulation of [15] is equivalent to UCS when Scenario (i) is considered with $L_{\max}(1) = 1$.

The largest cluster size considered is 4. $L_{\max}^{(A)}$ depends on the band: For our simulations we consider $L_{\max}^{(1)} \in \{1, 4\}$ and $L_{\max}^{(3)} \in \{1, 4\}$. For Band-2, only cellular transmission from macro BSs are allowed, and hence $L_{\max}^{(2)} = 1$. The number of all possible clusters of size greater than 4 is too large for any practical purpose. Besides, not all subsets of BSs are good candidates for being clusters. If a group of BSs are far from each other such that there is no user that is close enough to all of them, it is not necessary to include a cluster consisted of these BSs. With this intuition, we let each user pick the

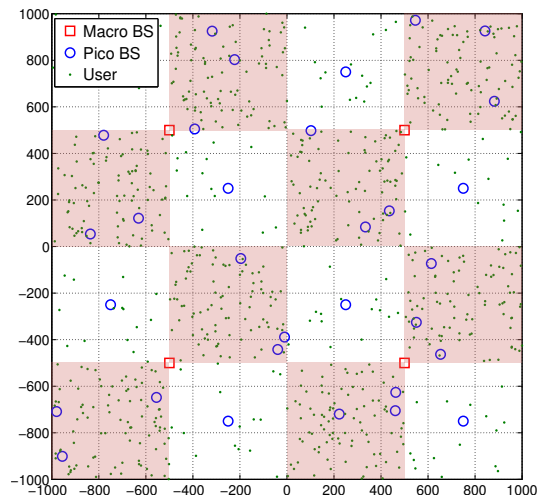


Fig. 2. The illustration of network deployment. The white grids are the regular areas, while the shadowed grids are hotspots.

strongest 8 BSs providing the largest signal strength to that user⁸. The potential clusters that can serve the user only include the BSs in these 8 BSs.

There is a one-to-one mapping between the log utility and the geometric mean of rates as $\left(\prod_{k=1}^K R_k\right)^{\frac{1}{K}} = \exp\left(\frac{1}{K} \sum_{k=1}^K \log R_k\right)$, thus we use geometric mean of rates as the metric for performance evaluation.

Fig. 3 show the geometric mean of rates using different approaches in scenarios (i) and (ii). We provide performance comparisons between the CVX solution (denoted as the UCS-NUM) of (5) and the solution of the dual subgradient based algorithm. The latter has almost the same performance as the NUM solution, which validates our analysis. We observe this also for our later simulations, hence the results of the dual algorithm are skipped in following figures for the sake of clarity. It can be seen when the solution to (5) is approximated by (15) with unique association, the utility loss is insignificant thanks to a very few number of fractional users (as shown in Prop. 2). Moreover, the proposed greedy VQ scheduling scheme provides performance close to the NUM solution, within 90% of the utility provided by the NUM solution in both scenarios (i) and (ii). Note that when cellular approach is used by UCS, the performance obtained by the NUM solution is feasible, rounding to a unique association and using VQ based scheduling is not necessary [15]. The performance of the optimal cellular transmission provided by [15] and of the Max-SINR association are also given for comparisons. We can observe that the UCS significantly improves the geometric mean of rates versus the optimal cellular performance and the max-SINR association, in both shared and orthogonal scenarios (about $1.6\times$ in the shared scenario and $1.35\times$ in the orthogonal scenario with respect to the optimal cellular result).

⁸We pick the strongest 8 BSs, since the performance of picking the strongest 9 BSs is almost the same as the 8-BS case, while the utility of picking the strongest 7 BSs is less than the 8-BS case.

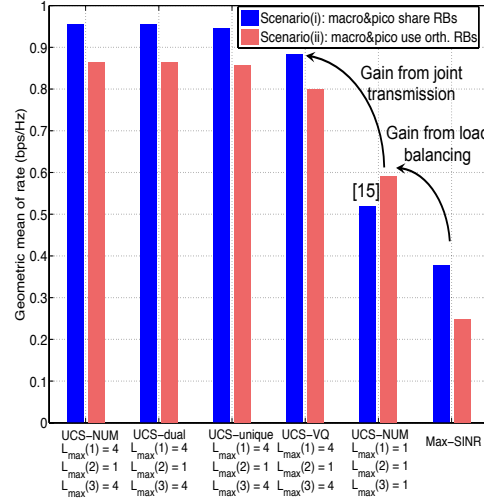


Fig. 3. The geometric mean of rates using different approaches ($\rho = 1$). The UCS with VQ based scheduling scheme provides a large performance gain (about $1.6\times$ and $1.35\times$ in the shared and orthogonal scenarios, respectively) versus the optimal cellular result.

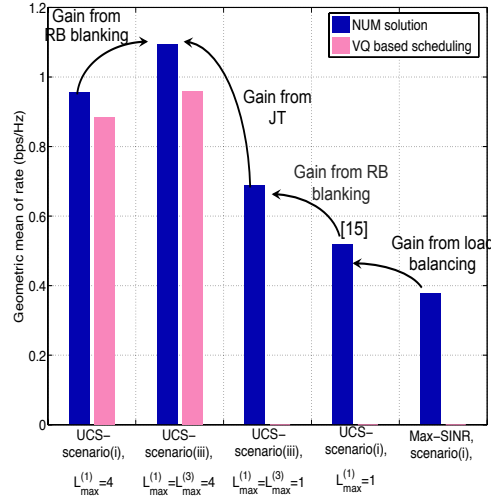


Fig. 4. The geometric mean of rates in the shared and RB blanking scenario ($\rho = 1$). RB blanking further improves the network performance.

In Fig. 4, we compare the performances of scenarios (i) and (iii). We can observe that RB blanking further improves the network utility.

We observe similar conclusions in Fig. 5, which shows the rate cumulative distribution function (CDF) with different approaches. We illustrate the results of the shared and RB blanking scenarios in the same figure, as RB blanking is essentially motivated from the shared scenario to manage the interference from macros to small cell users. Note that the rate here refers to long-term rate, which incorporating the resource sharing among users served by the same BS. The rate of bottom (the 10th percentile) users using the optimal user association with UCS in scenario (i) is about $2.2\times$ of the optimal cellular solution of [15]. The gain is even larger with UCS in scenario (ii).

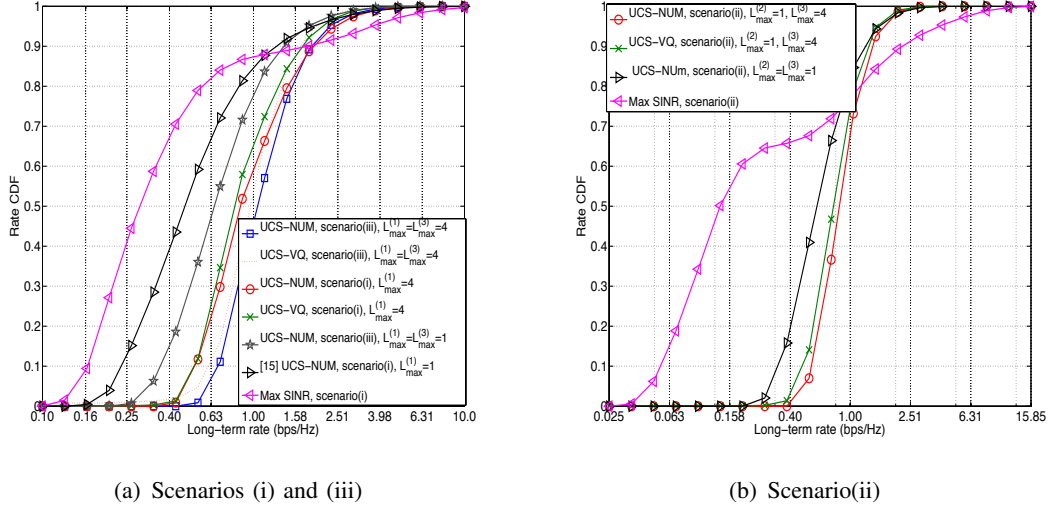


Fig. 5. The long-term rate CDF using different approaches ($\rho=1$). The rate of bottom (10th percentile) users using UCS is about $2.2\times$ of the cellular transmission case with optimal user association but without interference management.

The number of users served by different clusters with UCS is illustrated in Fig. 6. In the shared scenario with the max-SINR association, most users connect to the macro BSs, since the macro BSs have much larger transmit power than the small cell BSs. By load balancing, many users are offloaded to small BSs in the optimal cellular solution. In our proposed framework, all users are served by BS clusters with multiple BSs, which implies the potential gain using UCS. In the orthogonal scenario, there are no cross-tier interference and more users may get larger SINR from small BSs than macro BSs, hence more users connect to small cell BSs in the max-SINR association compared to the shared scenario. Due to the limited resources (20% RBs) available in macro BSs, more users are offloaded to small BSs using the load balancing approach in orthogonal cellular transmission case. For scenario (i), the percentage of fractional users is about 3.3% using UCS, and 1.2% in the case with optimal cellular. In the RB blanking scenario, the percentage of fractional users in the case using JT with RB blanking (Scenario (iii)) is about 2.5%, while the percentage of fractional users adopting cellular transmission with blanking is less than 1%. Thus, we can conclude that the number of fractional users in all cases is very small, which validates our analysis.

In Fig. 7, we show the geometric mean of rates versus different ρ . We observe that the performance gain using UCS decreases as ρ decreases, since the number of users that can be served by clusters decreases. When $\rho \geq 0.5$, the UCS can perform better than the cellular transmission. When ρ becomes smaller (e.g., $\rho = 0.25$, where all the considered clusters serve the same number of users as in the cellular transmission), the utility using UCS is almost the same as the cellular transmission. This implies that the gain from UCS increases as more UL pilot resources are available in the system. With limited UL

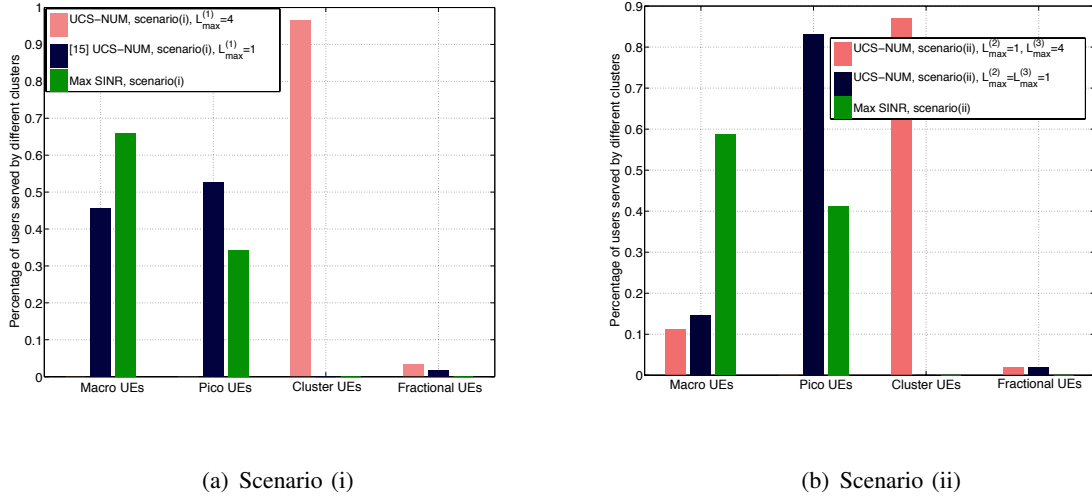


Fig. 6. The number of users served by different clusters ($\rho = 1$). Most users have unique association. The “Cluster UEs” refer to the users served by clusters of size larger than 1.

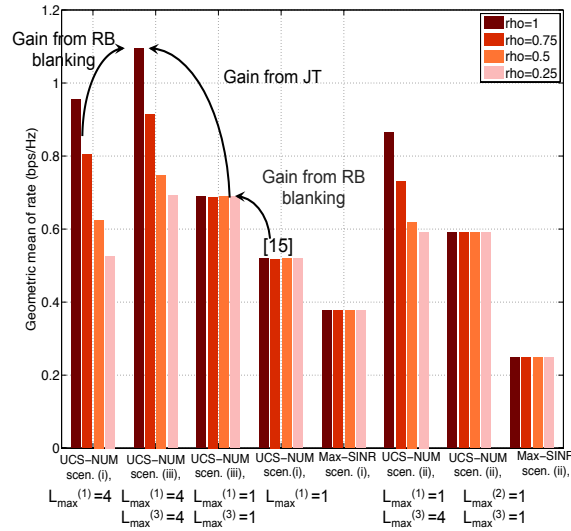


Fig. 7. The geometric mean of rates using different approaches versus ρ . As ρ decreases, the gain from JT decreases in both shared and orthogonal scenarios.

pilot resources, the gain from UCS would be quite small.

Fig. 8 illustrates the resource allocation for clusters of different sizes versus ρ in the RB blanking scenario. The macro BSs are off for about 65% RBs in the cellular transmission. In the case using JT with RB blanking (Scenario (iii)), as ρ decreases, the clusters serve less users, and more resources are allocated to the clusters of smaller sizes. When $\rho = 0.25$, all resources are allocated to single-BS clusters in normal RBs, and most of the resources are allocated to single-BS clusters in blank RBs. This again suggests that when the available pilot resources are strictly constrained, the gain from JT would be limited.

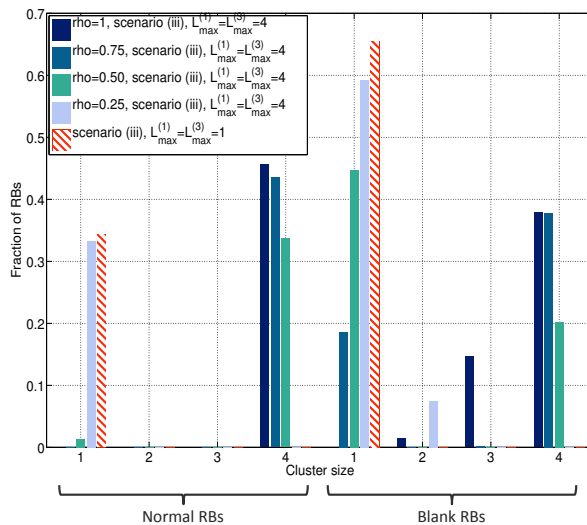


Fig. 8. The fraction of resources allocated to clusters of different sizes in the RB blanking scenario. As ρ decreases, more resources are allocated to clusters with smaller size.

VIII. CONCLUSION

In this paper, we investigate the joint optimization problem of user association and interference management in the massive MIMO HetNets. We consider both the JT and RB blanking approaches for interference management. We first provide the instantaneous rate from BS clusters by exploiting massive MIMO properties, namely the rate hardening and the independence of peak rate from the user scheduling. We then formulate a convex NUM problem to obtain the optimal user-specific BS clusters and the corresponding resource allocation. The unified formulation can be applied to both JT and blanking approaches, as well as the case where macro and small BSs use orthogonal resources. We further propose an efficient dual subgradient based algorithm, which is shown to converge towards the NUM solutions. We show that the NUM solution with JT may not be implementable by a feasible scheduler, and thus it provides an upper bound on the performance and can serve as a benchmark. Showing that most users connect to at most one cluster per RB in heavily loaded networks, we propose to approximate the NUM solution to a unique association, given which we propose a VQ based scheduling scheme to provide approximate but implementable results. Simulations show that the proposed scheduling scheme yields resource allocations that closely match the NUM solutions. More dynamic settings (e.g., users with high mobility) are left for future work. It is also of interest to theoretically bound the gap between the NUM solution and the results of the VQ based scheduling scheme.

APPENDIX A

PROOF OF THEOREM 1

We adopt similar techniques in the proof of Theorem 1 in [15]. Once the statement for one cluster size in one band is proven, the conclusion can be easily extended to general ATSS with various cluster sizes and multiple bands. Thus, we focus on clusters of size L in Band- A (in other words, subband L in Band- A). We ignore the index A for simplicity. All the clusters considered below satisfy $\mathcal{C} \subset \mathcal{B}^{(A)}$ and $|\mathcal{C}|=L$, unless otherwise specified. The set of feasible scheduling instants is denoted by \mathcal{F} , which includes vectors \mathbf{e} with element $e_{k\mathcal{C}} \in \{0, 1\}$, where $e_{k\mathcal{C}} = 1$ if user k connects to cluster \mathcal{C} and $e_{k\mathcal{C}} = 0$ otherwise. According to Defn. 3, the element in \mathcal{F} (i.e., \mathbf{e}) is consisted of $\{e_{k\mathcal{C}}\}$ satisfying that user k connects to at most one cluster and BS j serves at most $S_j(L)$ distinct users.

By time sharing among the feasible scheduling instants in \mathcal{F} , any fractional association in the convex hull of \mathcal{F} can be achieved in the long term. We denote the convex hull of \mathcal{F} by $X' = \text{conv}(\mathcal{F})$ and the set of activity fractions associated to clusters in A satisfying constraints in (5) by X , i.e.,

$$X = \left\{ x_{k\mathcal{C}} : \sum_{\mathcal{C}:j \in \mathcal{C}} \sum_{k \in \mathcal{U}} \frac{x_{k\mathcal{C}}}{S_j(L)} \leq 1, \sum_{\mathcal{C}} x_{k\mathcal{C}} \leq 1, x_{k\mathcal{C}} \geq 0, \forall k \in \mathcal{U}, \forall j \in \mathcal{B}^{(A)} \text{ and } \forall \mathcal{C} \subset \mathcal{B}^{(A)} \right\}.$$

It is easy to show that any feasible scheduling instants in \mathcal{F} satisfies the constraints (5b)-(5f), and thus $\mathcal{F} \subseteq X$. Note that X is convex. Thus, we have $X' = \text{conv}(\mathcal{F}) \subseteq X$.

As for the opposite direction (i.e., $X \not\subseteq X'$), we first define the *totally unimodular* (TU) matrix: every square submatrix of a TU matrix has determinant $+1$, -1 , or 0 . The Hoffman & Kruskal's (1956) Theorem claims that a matrix \mathbf{B} is TU if and only if for each integral vector \mathbf{b} , the *extreme points* of the polyhedron $\{\mathbf{z} : \mathbf{B}\mathbf{z} \leq \mathbf{b}, \mathbf{z} \geq 0\}$ are integral [48]. Denoting by $N_{\mathcal{C}L}^{(A)}$ the number of size- L clusters in Band- A , we let $\mathbf{x} = [\mathbf{x}_1^T, \mathbf{x}_2^T, \dots, \mathbf{x}_K^T]^T$ with $\mathbf{x}_k = [x_{k\mathcal{C}_1}, x_{k\mathcal{C}_2}, \dots, x_{k\mathcal{C}_{N_{\mathcal{C}L}^{(A)}}}]^T$, and $\mathbf{b} = [S_1(L), \dots, S_J(L), 1, \dots, 1]^T$ with size $(J+K) \times 1$. We let $\mathbf{B} = \begin{bmatrix} \mathbf{C} \\ \mathbf{D} \end{bmatrix}$, where the size of matrices \mathbf{C} and \mathbf{D} are $J \times (KN_{\mathcal{C}L}^{(A)})$ and $K \times (KN_{\mathcal{C}L}^{(A)})$, respectively. The element in j th row and $\left((k-1)N_{\mathcal{C}L}^{(A)} + i\right)$ th column of matrix \mathbf{B} is $1 \forall k \in \mathcal{U}$ if $j \in \mathcal{C}_i$, and 0 otherwise. The matrix \mathbf{C} has all elements being 1 . Recall that we consider large networks including the following type of cluster combination: $\{j_1, j_2\}$, $\{j_1, j_3\}$ and $\{j_2, j_3\}$ if $L_{\max}^{(A)} > 1$, where j_1, j_2 and j_3 are BS indexes. Then, \mathbf{B} with $L_{\max}^{(A)} > 1$ always includes the submatrix $\begin{bmatrix} 1 & 1 & 0 \\ 1 & 0 & 1 \\ 0 & 1 & 1 \end{bmatrix}$ whose determinant is -2 , and thus \mathbf{B} is not TU. According to the Hoffman & Kruskal's (1956) Theorem, there are some non-integer extreme points $\mathbf{v} \in X$ that cannot be characterized by a convex combination of any elements in \mathcal{F} . Thus, we have $\mathbf{v} \notin \text{conv}(\mathcal{F}) = X'$ and $X \not\subseteq X'$.

APPENDIX B

PROOF OF PROPOSITION 2

We use the techniques similar to the proof of Prop. 3 in [26], where a graph is used to represent the association, and KKT conditions (13) to restrict the structure of the graph. For a given cluster size L in Band- A , we denote the graph by G_1 , where nodes represent users, and edge between two nodes represents the BS cluster that serves the two users. Each node has an ID indicating the user index, while each edge has a color that identifies the BS cluster.

Recalling that constraints (5c) are inactive, we have $\theta_{kL}^{(A)} = 0, \forall k \in \mathcal{U}$. If there are two users k and m being served by size- L clusters \mathcal{C}_1 and \mathcal{C}_2 in Band- A (i.e., $x_{k\mathcal{C}_1}^{(A)} > 0, x_{k\mathcal{C}_2}^{(A)} > 0, x_{m\mathcal{C}_1}^{(A)} > 0, x_{m\mathcal{C}_2}^{(A)} > 0$), we have $R_k = \frac{r_{k\mathcal{C}_1}^{(A)}}{\sum_{j:j \in \mathcal{C}_1} \nu_{jL}^{(A)}/S_j(L)} = \frac{r_{k\mathcal{C}_2}^{(A)}}{\sum_{j:j \in \mathcal{C}_2} \nu_{jL}^{(A)}/S_j(L)}$ and $R_m = \frac{r_{m\mathcal{C}_1}^{(A)}}{\sum_{j:j \in \mathcal{C}_1} \nu_{jL}^{(A)}/S_j(L)} = \frac{r_{m\mathcal{C}_2}^{(A)}}{\sum_{j:j \in \mathcal{C}_2} \nu_{jL}^{(A)}/S_j(L)}$ from KKT condition (13), where $R_k = \sum_{A'=1}^3 \sum_{\mathcal{C}' \subset B(A')} x_{k\mathcal{C}'}^{(A')} r_{k\mathcal{C}'}^{(A')}$. Thus, we have

$$\frac{r_{k\mathcal{C}_1}^{(A)}}{r_{k\mathcal{C}_2}^{(A)}} = \frac{r_{m\mathcal{C}_1}^{(A)}}{r_{m\mathcal{C}_2}^{(A)}}, \quad (17)$$

which is true with probability 0. Therefore, it is almost sure that any two users can share at most one same cluster of size L in Band- A . Similarly, we consider an example of three users k, m, i and clusters $\mathcal{C}_1, \mathcal{C}_2, \mathcal{C}_3$. User k is associated to \mathcal{C}_1 and \mathcal{C}_2 , user m is associated to \mathcal{C}_1 and \mathcal{C}_3 , and user i is associated to \mathcal{C}_2 and \mathcal{C}_3 . We consider the following three cases:

- 1) If clusters $\mathcal{C}_1, \mathcal{C}_2$ and \mathcal{C}_3 are different, we have $\frac{r_{k\mathcal{C}_1}^{(A)}}{r_{k\mathcal{C}_2}^{(A)}} = \frac{\sum_{j:j \in \mathcal{C}_1} \nu_{jL}^{(A)}/S_j(L)}{\sum_{j:j \in \mathcal{C}_3} \nu_{jL}^{(A)}/S_j(L)} \frac{\sum_{j \in \mathcal{C}_3} \nu_{jL}^{(A)}/S_j(L)}{\sum_{j \in \mathcal{C}_2} \nu_{jL}^{(A)}/S_j(L)} = \frac{r_{m\mathcal{C}_1}^{(A)} r_{i\mathcal{C}_3}^{(A)}}{r_{m\mathcal{C}_3}^{(A)} r_{i\mathcal{C}_2}^{(A)}}$, which is true with probability 0.
- 2) If $\mathcal{C}_1 = \mathcal{C}_2 \neq \mathcal{C}_3$, we have that users m and i are served both by clusters \mathcal{C}_1 and \mathcal{C}_3 , which is true with probability 0 from (17).
- 3) If $\mathcal{C}_1 = \mathcal{C}_2 = \mathcal{C}_3$, we have that users k, m and i are served by the same cluster, which is possible. In this case, the graph becomes a *complete graph*.

Therefore, the graph G_1 with three users either contains a loop with the same color edges or no loop. We can get a similar result for graph G_1 with more than three users, where any subgraph formed by users served by the same BS cluster is a complete graph.

Thus, we generate a new graph, denoted by G_2 , where the node represents a cluster. Hence, G_2 has $N_{CL}^{(A)}$ nodes. There is an edge between two nodes in G_2 , if these two nodes (i.e., clusters) have a common vertex in G_1 (i.e., there is at least one user served by both these two clusters). Thus, the number of users who are served by more than one cluster is limited by the edge of G_2 . Any loop in

G_2 corresponds to a loop with more than one edge color in G_1 . Since there are no such colorful loops in G_1 , there is no loop in G_2 . In other words, G_2 is a tree. Thus, the maximal number of edges in G_2 (i.e., the maximal number of fractional users) is one less than the number of nodes (i.e., $N_{CL}^{(A)} - 1$).

APPENDIX C

IMPLEMENTATION ISSUES OF THE DUAL-SUBGRADIENT ALGORITHM

We let $L_{\max} = \max_A L_{\max}^{(A)}$, $N_{Cm} = \max_{L,A} N_{CL}^{(A)}$ and N_A be the number of operations. To solve (5) directly by CVX [46], we have the problem of size $O(N_{Cm}N_A L_{\max}K)$, which is dominated by the size of variables $x_{kC}^{(A)}$. On the other hand, as discussed below, the proposed algorithm has lower complexity. Let L_a be the maximal number of active cluster sizes over all bands (i.e., $\max_A |\{L : \lambda_{AL} > 0\}|$). The size of the LP (14) is $O(N_{Cm}N_A L_a \min\{N_{Cm} - 1, K\} + N_A L_a \max\{0, K - J + 1\})$, where the first term signifies the size of positive $x_{kC}^{(A)}$ for fractional users and the second term signifies the size of positive $x_{kC}^{(A)}$ for users with unique association. It is easy to check that the size of (14) is smaller than the size of (5). As shown in Sec. VII, the number of fractional users is very small (less than 3.5% K), and thus the size of (14) is much smaller (less than 3.5%) than (5). Moreover, the size of (14) can be further reduced when L_a/L_{\max} is small (e.g., only 2 active cluster sizes among 4 possible sizes in Sec. VII). The fast convergence in the first part (i.e., steps (8)-(11)) of the algorithm (less than 60 iterations in our simulation) along with the low complexity per iteration, and the reduced size of (14) makes that the proposed algorithm can be more efficient than CVX for larger networks.

REFERENCES

- [1] J. G. Andrews, "Seven ways that HetNets are a cellular paradigm shift," *IEEE Comm. Mag.*, vol. 51, pp. 136–144, Mar. 2013.
- [2] J. G. Andrews, S. Buzzi, W. Choi, S. V. Hanly, A. Lozano, A. C. K. Soong, and J. C. Zhang, "What will 5G be?," *IEEE Journal on Sel. Areas in Communications*, vol. 32, pp. 1065–1082, June 2014.
- [3] F. Boccardi, R. W. Heath, A. Lozano, T. L. Marzetta, and P. Popovski, "Five disruptive technology directions for 5G," *IEEE Comm. Mag.*, vol. 52, pp. 74–80, Feb. 2014.
- [4] T. L. Marzetta, "Noncooperative cellular wireless with unlimited numbers of base station antennas," *IEEE Trans. on Wireless Communications*, vol. 9, pp. 3590–3600, Nov. 2010.
- [5] J. Hoydis, S. Ten Brink, M. Debbah, *et al.*, "Massive MIMO in the UL/DL of cellular networks: How many antennas do we need?," *IEEE Journal on Sel. Areas in Communications*, vol. 31, pp. 160–171, Feb. 2013.
- [6] E. Larsson, O. Edfors, F. Tufvesson, and T. Marzetta, "Massive MIMO for next generation wireless systems," *IEEE Comm. Mag.*, vol. 52, pp. 186–195, Feb. 2014.
- [7] 3GPP, "Technical specification group radio access network; Small cell enhancements for E-UTRA and E-UTRAN," *TR 36.872, V12.1.0*, Dec. 2013.

- [8] J. G. Andrews, S. Singh, Q. Ye, X. Lin, and H. Dhillon, "An overview of load balancing in hetnets: Old myths and open problems," *IEEE Wireless Communications*, vol. 21, pp. 18–25, Apr. 2014.
- [9] S. Singh, H. S. Dhillon, and J. G. Andrews, "Offloading in heterogeneous networks: Modeling, analysis, and design insights," *IEEE Trans. on Wireless Communications*, vol. 12, pp. 2484–2497, May 2013.
- [10] H. S. Jo, Y. J. Sang, P. Xia, and J. G. Andrews, "Heterogeneous cellular networks with flexible cell association: a comprehensive downlink SINR analysis," *IEEE Trans. on Wireless Communications*, vol. 11, pp. 3484–3495, Oct. 2012.
- [11] E. Aryafar, A. Keshavarz-Haddad, M. Wang, and M. Chiang, "RAT selection games in HetNets," in *Proc., IEEE INFOCOM*, pp. 998–1006, Apr. 2013.
- [12] A. Damnjanovic, J. Montojo, Y. Wei, T. Ji, T. Luo, M. Vajapeyam, T. Yoo, O. Song, and D. Malladi, "A survey on 3GPP heterogeneous networks," *IEEE Wireless Communications Magazine*, vol. 18, pp. 10–21, June 2011.
- [13] A. Ghosh, N. Mangalvedhe, R. Ratasuk, B. Mondal, M. Cudak, E. Visotsky, T. A. Thomas, J. G. Andrews, *et al.*, "Heterogeneous cellular networks: From theory to practice," *IEEE Comm. Mag.*, vol. 50, pp. 54–64, June 2012.
- [14] Q. Ye, B. Rong, Y. Chen, M. Al-Shalash, C. Caramanis, and J. Andrews, "User association for load balancing in heterogeneous cellular networks," *IEEE Trans. on Wireless Communications*, vol. 12, pp. 2706–2716, June 2013.
- [15] D. Bethanabhotla, O. Y. Bursalioglu, H. C. Papadopoulos, and G. Caire, "Optimal user-cell association for massive MIMO wireless networks," *submitted to IEEE Trans. Wireless Comm.*, Feb. 2015. Available at arXiv: <http://arxiv.org/abs/1407.6731>.
- [16] D. Gesbert, S. Hanly, H. Huang, S. Shamai Shitz, O. Simeone, and W. Yu, "Multi-cell MIMO cooperative networks: A new look at interference," *IEEE Journal on Sel. Areas in Communications*, vol. 28, pp. 1380–1408, Dec. 2010.
- [17] M. Sawahashi, Y. Kishiyama, A. Morimoto, D. Nishikawa, and M. Tanno, "Coordinated multipoint transmission/reception techniques for LTE-Advanced [coordinated and distributed MIMO]," *IEEE Wireless Communications*, vol. 17, pp. 26–34, June 2010.
- [18] D. Lee, H. Seo, B. Clerckx, E. Hardouin, D. Mazzaresse, S. Nagata, and K. Sayana, "Coordinated multipoint transmission and reception in LTE-Advanced: deployment scenarios and operational challenges," *IEEE Comm. Mag.*, vol. 50, pp. 148–155, Feb. 2012.
- [19] P. Marsch and G. Fettweis, "Static clustering for cooperative multi-point (CoMP) in mobile communications," in *Proc., IEEE Intl. Conf. on Communications*, pp. 1–6, June 2011.
- [20] J. Li, T. Svensson, C. Botella, T. Eriksson, X. Xu, and X. Chen, "Joint scheduling and power control in coordinated multi-point clusters," in *Proc., IEEE Veh. Technology Conf.*, pp. 1–5, Sep. 2011.
- [21] J. Zhao, T. Q. S. Quek, and Z. Lei, "Coordinated multipoint transmission with limited backhaul data transfer," *IEEE Trans. on Wireless Communications*, vol. 12, pp. 2762–2775, June 2013.
- [22] Y. Du and G. de Veciana, "'Wireless networks without edges': Dynamic radio resource clustering and user scheduling," in *Proc., IEEE INFOCOM*, pp. 1321–1329, Apr. 2014.
- [23] H. Huh, G. Caire, H. C. Papadopoulos, and S. A. Ramprasad, "Achieving large spectral efficiency with TDD and not-so-many base-station antennas," in *IEEE APWC*, pp. 1346–1349, Sep. 2011.
- [24] D. Lopez-Perez *et al.*, "Enhanced intercell interference coordination challenges in heterogeneous networks," *IEEE Wireless Communications*, vol. 18, pp. 22–30, June 2011.
- [25] S. Vasudevan, R. Pupala, and K. Sivanesan, "Dynamic eICIC - a proactive strategy for improving spectral efficiencies of heterogeneous LTE cellular networks by leveraging user mobility and traffic dynamics," *IEEE Trans. on Wireless Communications*, vol. 12, pp. 4956–4969, Oct. 2013.
- [26] Q. Ye, M. Al-Shalash, C. Caramanis, and J. G. Andrews, "On/off macrocells and load balancing in heterogeneous cellular networks," in *Proc., IEEE Globecom*, pp. 3814–3819, Dec. 2013.

- [27] A. Bedekar and R. Agrawal, "Optimal muting and load balancing for eICIC," in *Intl. Symposium on Modeling and Optimization in Mobile, Ad Hoc and Wireless Networks (WiOpt)*, pp. 280–287, May 2013.
- [28] J. Ghimire and C. Rosenberg, "Resource allocation, transmission coordination and user association in heterogeneous networks: A flow-based unified approach," *IEEE Trans. on Wireless Communications*, vol. 12, pp. 1340–1351, Mar. 2013.
- [29] S. Deb, P. Monogioudis, J. Miernik, and J. P. Seymour, "Algorithms for enhanced inter-cell interference coordination (eICIC) in LTE hetnets," *IEEE/ACM Trans. on Networking*, vol. 22, pp. 137–150, Feb. 2014.
- [30] S. Singh and J. G. Andrews, "Joint resource partitioning and offloading in heterogeneous cellular networks," *IEEE Trans. on Wireless Communications*, vol. 13, pp. 888–901, Feb. 2014.
- [31] E. Hossain, M. Rasti, H. Tabassum, and A. Abdelnasser, "Evolution toward 5G multi-tier cellular wireless networks: An interference management perspective," *IEEE Wireless Communications*, vol. 21, pp. 118–127, June 2014.
- [32] S. Shakkottai, T. S. Rappaport, and P. C. Karlsson, "Cross-layer design for wireless networks," *IEEE Comm. Mag.*, vol. 41, pp. 74–80, Oct. 2003.
- [33] X. Lin, N. Shroff, and R. Srikant, "A tutorial on cross-layer optimization in wireless networks," *IEEE Journal on Sel. Areas in Communications*, vol. 24, pp. 1452–1463, Aug. 2006.
- [34] A. L. Stolyar, "On the asymptotic optimality of the gradient scheduling algorithm for multiuser throughput allocation," *Operations research*, vol. 53, pp. 12–25, Feb. 2005.
- [35] L. Chen, S. Low, M. Chiang, and J. Doyle, "Cross-layer congestion control, routing and scheduling design in ad hoc wireless networks," in *Proc., IEEE INFOCOM*, pp. 1–13, Apr. 2006.
- [36] G. R. Gupta, S. Sanghavi, and N. B. Shroff, "Node weighted scheduling," in *ACM SIGMETRICS*, vol. 37, pp. 97–108, June 2009.
- [37] A. Berger, J. Gross, and T. Harks, "The k-constrained bipartite matching problem: Approximation algorithms and applications to wireless networks," in *Proc., IEEE INFOCOM*, pp. 1–9, Mar. 2010.
- [38] Q. Ye, O. Y. Bursalioglu, and H. Papadopoulos, "Harmonized cellular and distributed massive MIMO: Load balancing and scheduling," in *Proc., IEEE Globecom*, Dec. 2015.
- [39] G. Caire, N. Jindal, M. Kobayashi, and N. Ravindran, "Multiuser MIMO achievable rates with downlink training and channel state feedback," *IEEE Trans. on Info. Theory*, vol. 56, pp. 2845–2866, June 2010.
- [40] J. Zhang, R. Chen, J. G. Andrews, A. Ghosh, and R. W. Heath, "Networked MIMO with clustered linear precoding," *IEEE Trans. on Wireless Communications*, vol. 8, pp. 1910–1921, Apr. 2009.
- [41] H. Huh, A. M. Tulino, and G. Caire, "Network MIMO with linear zero-forcing beamforming: Large system analysis, impact of channel estimation, and reduced-complexity scheduling," *IEEE Trans. on Info. Theory*, vol. 58, pp. 2911–2934, May 2012.
- [42] Y.-G. Lim, C.-B. Chae, and G. Caire, "Performance analysis of massive MIMO for cell-boundary users," *accepted to IEEE Trans. on Communications*, Sep. 2013. Available at arXiv: <http://arxiv.org/abs/1309.7817>.
- [43] S. Stanczak, M. Wiczanowski, and H. Boche, *Fundamentals of Resource Allocation in Wireless Networks: Theory and Algorithms*, vol. 3. Springer Verlag, 2009.
- [44] D. Tse and P. Viswanath, *Fundamentals of Wireless Communication*. Cambridge university press, 2005.
- [45] D. P. Bertsekas, *Convex Optimization Theory*. Athena Scientific, 2009.
- [46] M. Grant, S. Boyd, and Y. Ye, "CVX: Matlab software for disciplined convex programming," 2009. Available: <http://cvxr.com/cvx/>.
- [47] H. Shirani-Mehr, G. Caire, and M. J. Neely, "MIMO downlink scheduling with non-perfect channel state knowledge," *IEEE Trans. on Communications*, vol. 58, pp. 2055–2066, July 2010.
- [48] A. Schrijver, *Theory of Linear and Integer Programming*. John Wiley & Sons, 1998.